nature portfolio

https://doi.org/10.1038/s43017-022-00263-2

Supplementary information

The evolution of the North Atlantic Meridional Overturning Circulation since 1980

In the format provided by the authors and unedited

Appendix: Data used

All AMOC reconstructions and proxies are listed in Table S1.

Reanalyses

The ensemble mean and standard deviation were calculated from reanalyses participating in ref[1], with the exception of ORAS5 and GECCO2 which were shown to have problems replicating AMOC variability.

Forced models

The ensemble mean and standard deviation were calculated from forced models participating in OMIP2[2]. Models used were those available to download: CESM2, CNRM-CM6-1, EC-Earth3, FGOALS-f3-L, NorESM2-LM. Results from another forced model study[3] are also shown in Figure S1 at 26.5^{o}N (data from other latitudes was not available). There is qualitative agreement between the two ensembles, however the second ensemble has a less pronounced peak around year 2006.

Coupled models

The coupled models were taken from CMIP6 preindustrial experiments[4–13], historical experiments[14–33] and experiments with the future scenario ssp585[34–47]

Type	Name	Method	Latitude	Depth/density space	years used
Observations	OVIDE[48]	TW from ocean floats and satellite altimetry, Ekman from reanalysis winds	40-60^{o}N	density	1993-2016
Observations	45^{o}N[49]	TW from ocean floats and satellite altimetry	45^{o}N	density and depth	1993-2018
Observations	Surf flux[49]	Implied AMOC from water mass transformation, fluxes from reanalyses	45^{o}N	density	1988-2015
Observations	41^{o}N[50]	TW from ocean floats and satellite altimetry, Ekman from reanalysis winds	41^{o}N	depth	1993-2017
Observations	RAPID[51,52]	TW from moorings, boundary currents from submarine cable, Ekman from satellite winds	26.5^{o}N	depth	2005-2018
Observations	26.5^{o}N[53]	Extension of RAPID using relationships with altimetry	26.5^{o}N	depth	1993-2019
Reanalyses	Reanalyses[1]	Ensemble mean and spread from ensemble of reanalyses	26.5,50^{o}N	depth	1993-2016
Forced models	Forced models[54]	Ensemble mean and spread from ensemble of ocean models	26.5,50^{o}N	depth	1960-2019
Proxies	LSD[55]	Labrador sea density (1000-2500m,35-60^{o}W,50-65^{o}N mean) using EN4[56]	subpolar	-	1980-2020
Proxies	SS[57]	Sortable silt, proxy for deep west boundary current	35^{o}N	-	1980-2003
Proxies	SL[58,59]	Sea level difference on east coast of USA (26-34^{o}N minus 36.5-42^{o}N)	intergyre	-	1980-2016
Proxies	AMV1[60]	SST (0-60^{o}N,50^{o}W-10^{o}E mean minus global mean) using EN4[56]	-	-	1980-2020
Proxies	AMV2[61]	SST (40-60^{o}N,50^{o}W-10^{o}E mean minus global mean) using EN4[56]	-	-	1980-2020
Proxies	SST[62]	SST in subpolar gyre region (as in ref[63]) minus NH mean using EN4[56]	-	-	1980-2020
Proxies	TSUB[64,65]	Temperature at 400m (50-60N, 30-50W mean minus 35-46N, 40-70W) using EN4[56]	-	-	1980-2020
Proxies	UOHC[64,65]	OHC (0-700m, 50-60N, 30-50W mean minus 35-46N, 40-70W mean) using EN4[56]	-	-	1980-2020

Supplementary Table 1. AMOC reconstructions and proxies used in this study. Here TW is thermal wind and OHC ocean heat content.

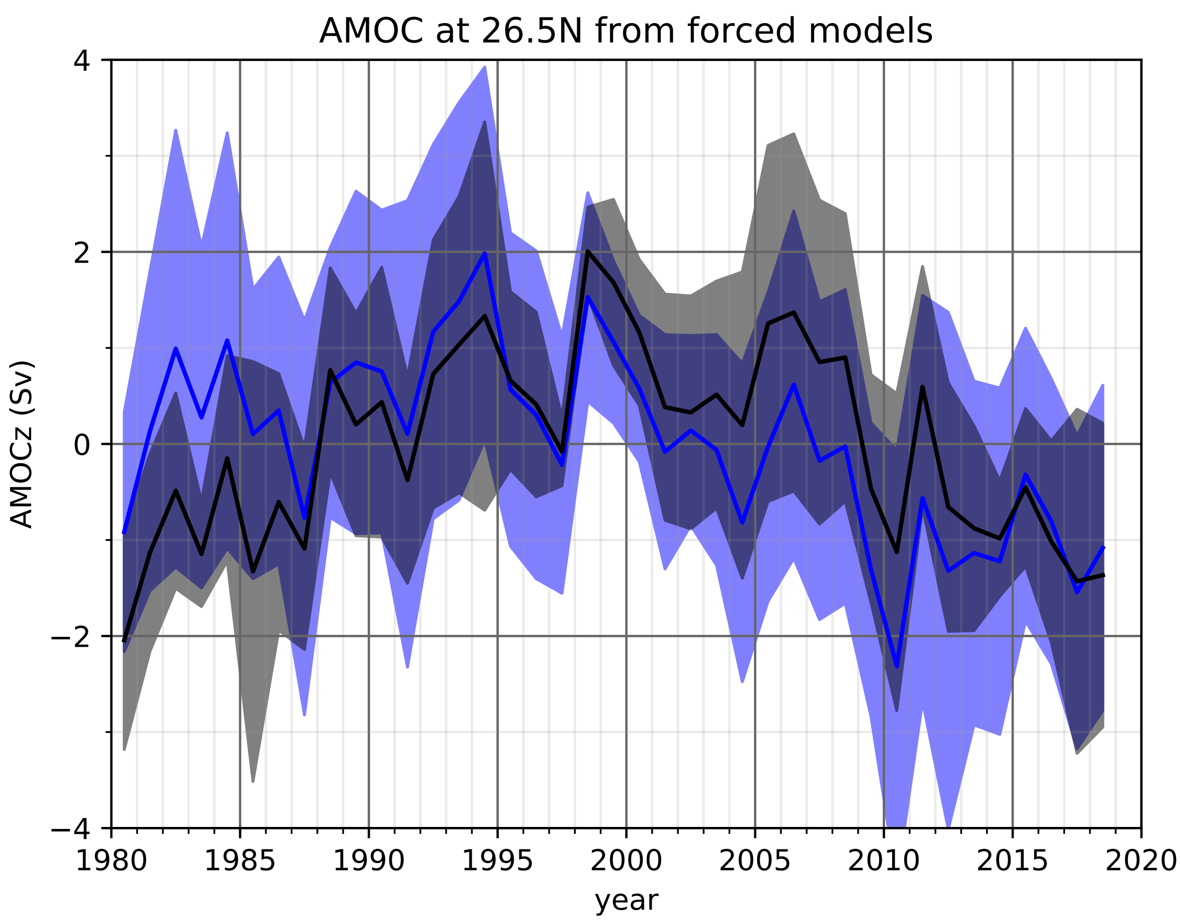

Supplementary Figure 1. Annual mean AMOC anomalies at 26.5^{o}N from forced models participating in OMIP2[2] (black), and from forced models from ref[3]. Lines are ensemble means with shading showing 2 times the standard deviation across models.

References

1. Jackson, L. C. *et al.* The mean state and variability of the north atlantic circulation: A perspective from ocean reanalyses. *J. Geophys. Res. Ocean.* **124**, 9141–9170, DOI: https://doi.org/10.1029/2019JC015210 (2019).
2. Tsujino, H. *et al.* Evaluation of global ocean–sea-ice model simulations based on the experimental protocols of the Ocean Model Intercomparison Project phase 2 (OMIP-2). *Geosci. Model. Dev. Discuss.* **2020**, 1–86, DOI: 10.5194/gmd-2019-363 (2020).
3. Chassignet, E. P. *et al.* Impact of horizontal resolution on global ocean–sea ice model simulations based on the experimental protocols of the ocean model intercomparison project phase 2 (omip-2). *Geosci. Model. Dev.* **13**, 4595–4637, DOI: 10.5194/gmd-13-4595-2020 (2020).
4. for Space Studies (NASA/GISS), N. G. I. Nasa-giss giss-e2-2-g model output prepared for cmip6 cmip picontrol, DOI: 10.22033/ESGF/CMIP6.7382 (2019).
5. Wieners, K.-H. *et al.* Mpi-m mpi-esm1.2-lr model output prepared for cmip6 cmip picontrol, DOI: 10.22033/ESGF/CMIP6.6675 (2019).
6. Swart, N. C. *et al.* Cccma canesm5 model output prepared for cmip6 cmip picontrol, DOI: 10.22033/ESGF/CMIP6.3673 (2019).

7. Volodin, E. *et al.* Inm inm-cm5-0 model output prepared for cmip6 cmip picontrol, DOI: 10.22033/ESGF/CMIP6.5081 (2019).

8. Dix, M. *et al.* Csiro-arccss access-cm2 model output prepared for cmip6 cmip picontrol, DOI: 10.22033/ESGF/CMIP6.4311 (2019).

9. Li, L. Cas fgoals-g3 model output prepared for cmip6 cmip picontrol, DOI: 10.22033/ESGF/CMIP6.3448 (2019).

10. Tatebe, H. & Watanabe, M. Miroc miroc6 model output prepared for cmip6 cmip picontrol, DOI: 10.22033/ESGF/CMIP6.5711 (2018).

11. Bethke, I. *et al.* Ncc norcpm1 model output prepared for cmip6 cmip picontrol, DOI: 10.22033/ESGF/CMIP6.10896 (2019).

12. Danabasoglu, G., Lawrence, D., Lindsay, K., Lipscomb, W. & Strand, G. Ncar cesm2 model output prepared for cmip6 cmip picontrol, DOI: 10.22033/ESGF/CMIP6.7733 (2019).

13. Yukimoto, S. *et al.* Mri mri-esm2.0 model output prepared for cmip6 cmip picontrol, DOI: 10.22033/ESGF/CMIP6.6900 (2019).

14. Jungclaus, J. *et al.* Mpi-m mpi-esm1.2-hr model output prepared for cmip6 cmip historical, DOI: 10.22033/ESGF/CMIP6.6594 (2019).

15. Chai, Z. Cas cas-esm1.0 model output prepared for cmip6 cmip historical, DOI: 10.22033/ESGF/CMIP6.3353 (2020).

16. Dix, M. *et al.* Csiro-arccss access-cm2 model output prepared for cmip6 cmip historical, DOI: 10.22033/ESGF/CMIP6.4271 (2019).

17. Ziehn, T. *et al.* Csiro access-esm1.5 model output prepared for cmip6 cmip historical, DOI: 10.22033/ESGF/CMIP6.4272 (2019).

18. Tatebe, H. & Watanabe, M. Miroc miroc6 model output prepared for cmip6 cmip historical, DOI: 10.22033/ESGF/CMIP6.5603 (2018).

19. Swart, N. C. *et al.* Cccma canesm5 model output prepared for cmip6 cmip historical, DOI: 10.22033/ESGF/CMIP6.3610 (2019).

20. Park, S. & Shin, J. Snu sam0-unicon model output prepared for cmip6 cmip historical, DOI: 10.22033/ESGF/CMIP6.7789 (2019).

21. Danabasoglu, G. Ncar cesm2-waccm-fv2 model output prepared for cmip6 cmip historical, DOI: 10.22033/ESGF/CMIP6.11298 (2019).

22. Volodin, E. *et al.* Inm inm-cm4-8 model output prepared for cmip6 cmip historical, DOI: 10.22033/ESGF/CMIP6.5069 (2019).

23. Danabasoglu, G. Ncar cesm2-waccm model output prepared for cmip6 cmip historical, DOI: 10.22033/ESGF/CMIP6.10071 (2019).

24. YU, Y. Cas fgoals-f3-l model output prepared for cmip6 cmip historical, DOI: 10.22033/ESGF/CMIP6.3355 (2019).

25. Yukimoto, S. *et al.* Mri mri-esm2.0 model output prepared for cmip6 cmip historical, DOI: 10.22033/ESGF/CMIP6.6842 (2019).

26. Seland, y. *et al.* Ncc noresm2-lm model output prepared for cmip6 cmip historical, DOI: 10.22033/ESGF/CMIP6.8036 (2019).

27. Neubauer, D. *et al.* Hammoz-consortium mpi-esm1.2-ham model output prepared for cmip6 cmip historical, DOI: 10.22033/ESGF/CMIP6.5016 (2019).

28. Danabasoglu, G. Ncar cesm2-fv2 model output prepared for cmip6 cmip historical, DOI: 10.22033/ESGF/CMIP6.11297 (2019).

29. Bethke, I. *et al.* Ncc norcpm1 model output prepared for cmip6 cmip historical, DOI: 10.22033/ESGF/CMIP6.10894 (2019).

30. Wieners, K.-H. *et al.* Mpi-m mpi-esm1.2-lr model output prepared for cmip6 cmip historical, DOI: 10.22033/ESGF/CMIP6.6595 (2019).

31. Volodin, E. *et al.* Inm inm-cm5-0 model output prepared for cmip6 cmip historical, DOI: 10.22033/ESGF/CMIP6.5070 (2019).

32. Danabasoglu, G. Ncar cesm2 model output prepared for cmip6 cmip historical, DOI: 10.22033/ESGF/CMIP6.7627 (2019).

33. Bentsen, M. *et al.* Ncc noresm2-mm model output prepared for cmip6 cmip historical, DOI: 10.22033/ESGF/CMIP6.8040 (2019).

34. Dix, M. *et al.* Csiro-arccss access-cm2 model output prepared for cmip6 scenariomip ssp585, DOI: 10.22033/ESGF/CMIP6.4332 (2019).

35. Seland, y. *et al.* Ncc noresm2-lm model output prepared for cmip6 scenariomip ssp585, DOI: 10.22033/ESGF/CMIP6.8319 (2019).

36. Bentsen, M. *et al.* Ncc noresm2-mm model output prepared for cmip6 scenariomip ssp585, DOI: 10.22033/ESGF/CMIP6.8321 (2019).

37. YU, Y. Cas fgoals-f3-l model output prepared for cmip6 scenariomip ssp585, DOI: 10.22033/ESGF/CMIP6.3502 (2019).

38. Li, L. Cas fgoals-g3 model output prepared for cmip6 scenariomip ssp585, DOI: 10.22033/ESGF/CMIP6.3503 (2019).

39. Ziehn, T. *et al.* Csiro access-esm1.5 model output prepared for cmip6 scenariomip ssp585, DOI: 10.22033/ESGF/CMIP6.4333 (2019).

40. Schupfner, M. *et al.* Dkrz mpi-esm1.2-hr model output prepared for cmip6 scenariomip ssp585, DOI: 10.22033/ESGF/CMIP6.4403 (2019).

41. Volodin, E. *et al.* Inm inm-cm4-8 model output prepared for cmip6 scenariomip ssp585, DOI: 10.22033/ESGF/CMIP6.12337 (2019).

42. Volodin, E. *et al.* Inm inm-cm5-0 model output prepared for cmip6 scenariomip ssp585, DOI: 10.22033/ESGF/CMIP6.12338 (2019).

43. Shiogama, H., Abe, M. & Tatebe, H. Miroc miroc6 model output prepared for cmip6 scenariomip ssp585, DOI: 10.22033/ESGF/CMIP6.5771 (2019).

44. Wieners, K.-H. *et al.* Mpi-m mpi-esm1.2-lr model output prepared for cmip6 scenariomip ssp585, DOI: 10.22033/ESGF/CMIP6.6705 (2019).

45. Yukimoto, S. *et al.* Mri mri-esm2.0 model output prepared for cmip6 scenariomip ssp585, DOI: 10.22033/ESGF/CMIP6.6929 (2019).

46. Danabasoglu, G. Ncar cesm2-waccm model output prepared for cmip6 scenariomip ssp585, DOI: 10.22033/ESGF/CMIP6.10115 (2019).

47. Swart, N. C. *et al.* Cccma canesm5 model output prepared for cmip6 scenariomip ssp585, DOI: 10.22033/ESGF/CMIP6.3696 (2019).

48. Mercier, H. *et al.* Variability of the meridional overturning circulation at the greenland–portugal ovide section from 1993 to 2010. *Prog. Oceanogr.* **132**, 250 – 261, DOI: https://doi.org/10.1016/j.pocean.2013.11.001 (2015).

49. Desbruyères, D., Mercier, H., Maze, G. & Daniault, N. Surface predictor of overturning circulation and heat content change in the subpolar north atlantic. *Ocean. Sci.* **15**, 809–817, DOI: 10.5194/os-15-809-2019 (2019).

50. Willis, J. K. Can in situ floats and satellite altimeters detect long-term changes in atlantic ocean overturning? geophys. res. lett., 37, l06602, doi:10.1029/2010gl042372. *Geophys. Res. Lett.* **37**, L06602, DOI: 10.1029/2010GL042372 (2010).

51. McCarthy, G. D. *et al.* Measuring the Atlantic meridional overturning circulation at 26°N. *Prog. Oceanogr.* **130**, 91–111, DOI: 10.1016/j.pocean.2014.10.006 (2015).

52. Moat, B. I. *et al.* Atlantic meridional overturning circulation observed by the rapid-mocha-wbts (rapid-meridional overturning circulation and heatflux array-western boundary time series) array at 26n from 2004 to 2018 (v2018.2), DOI: 10.5285/aa57e879-4cca-28b6-e053-6c86abc02de5 (2020).

53. Sanchez-Franks, A., Frajka-Williams, E., Moat, B. I. & Smeed, D. A. A dynamically based method for estimating the atlantic meridional overturning circulation at 26n from satellite altimetry. *Ocean. Sci.* **17**, 1321–1340, DOI: 10.5194/os-17-1321-2021 (2021).

54. Tsujino, H. *et al.* JRA-55 based surface dataset for driving ocean–sea-ice models (JRA55-do). *Ocean. Model.* **130**, 79–139, DOI: 10.1016/j.ocemod.2018.07.002 (2018).

55. Robson, J., Ortega, P. & Sutton, R. A reversal of climatic trends in the North Atlantic since 2005. *Nat. Geosci.* **9**, 513–517, DOI: 10.1038/ngeo2727 (2016).

56. Good, S. A., Martin, M. J. & Rayner, N. A. EN4: Quality controlled ocean temperature and salinity profiles and monthly objective analyses with uncertainty estimates. *J. Geophys. Res.* **118**, 6704–6716 (2013).

57. Thornalley, D. J. R. *et al.* Anomalously weak labrador sea convection and atlantic overturning during the past 150 years. *Nature* **556**, 227–230, DOI: 10.1038/s41586-018-0007-4 (2018).

58. MacCarthy, G. D., Haigh, I. D., Hirschi, J. J.-M., Grist, J. P. & Smeed, D. A. Ocean impact on decadal atlantic climate variability revealed by sea-level observations. *Nature* **521**, 508–510 (2015).

59. Diabaté, S. T. *et al.* Western boundary circulation and coastal sea-level variability in northern hemisphere oceans. *Ocean. Sci.* **17**, 1449–1471, DOI: 10.5194/os-17-1449-2021 (2021).

60. Latif, M. *et al.* Reconstructing, monitoring, and predicting multidecadal-scale changes in the north atlantic thermohaline circulation with sea surface temperature. *J. Clim.* **17**, 1605–1614, DOI: 10.1175/1520-0442(2004)017<1605:RMAPMC>2.0.CO;2 (2004).

61. Msadek, R., Dixon, K. W., Delworth, T. L. & Hurlin, W. Assessing the predictability of the atlantic meridional overturning circulation and associated fingerprints. *Geophys. Res. Lett* **37**, L19608, DOI: 10.1029/2010GL044517 (2010).

62. Rahmstorf, S. *et al.* Exceptional twentieth-century slowdown in Atlantic Ocean overturning circulation. *Nat. Clim. Chang.* **5**, 475–480, DOI: 10.1038/nclimate2554 (2015).

63. Caesar, L., Rahmstorf, S., Robinson, A., Feulner, G. & Saba, V. Observed fingerprint of a weakening atlantic ocean overturning circulation. *Nature* **556**, 191–196, DOI: 10.1038/s41586-018-0006-5 (2018).

64. Zhang, R. Coherent surface-subsurface fingerprint of the Atlantic meridional overturning circulation. *Geophys. Res. Lett.* **35**, L20705+, DOI: 10.1029/2008gl035463 (2008).

65. Zhang, J. & Zhang, R. On the evolution of atlantic meridional overturning circulation fingerprint and implications for decadal predictability in the north atlantic. *Geophys. Res. Lett.* **42**, 5419–5426, DOI: 10.1002/2015GL064596 (2015).